Astronomical and Astrophysical Transactions (*AApTr*), 2025, Vol. 35, Issue 1, pp. 29–42,
ISSN 1055-6796, Photocopying permitted by license only, ©Cambridge Scientific Publishers

Study of the period changes in SU Hor – an RR Lyrae type star with the Blazhko effect

L.N. Berdnikov[1,*], A.Y. Kniazev[1,2,3], A.K. Dambis[1], E.N. Pastukhova[4]

[1]*Sternberg Astronomical Institute, Moscow State University, Universitetskii Pr. 13, Moscow, 119992 Russia*
[2]*South African Astronomical Observatory, P.O. Box 9, Observatory, Cape Town, 7935 South Africa*
[3]*Southern African Large Telescope, P.O. Box 9, Observatory, Cape Town, 7935 South Africa*
[4]*Institute of Astronomy, Russian Academy of Sciences, 48 Pyatnitskaya Street, Moscow, 119017 Russia*

Received 23 April, 2025; accepted 28 April, 2025

In 2012–2014 we acquired 3965 CCD BVI_c frames for the RR Lyrae type variable SU Hor with the 76-cm telescope of the South African Astronomical Observatory (SAAO) Sutherland and 1-m telescopes of Las Cumbres Observatory Global Telescope network (LCOGT). Our observations confirmed the presence of the Blazhko effect, which we suspected earlier, and allowed us to determine the Blazhko period, $P_{Bl} = 32.^d27 \pm 0.^d03$. We used all available observations to construct the $O-C$ diagram spanning a 134-year long time interval and discovered for the first time the evolutionary period change at a rate of $dp/dt = -0.0814 \pm 0.0016$ s/year.

Keywords: Stars: variables: RR Lyrae; stars: oscillations; techniques: photometric; galaxies: spirals

1 Introduction

The high luminosities and old ages of RR Lyrae type variables make them ideal distance indicators and tracers for the study of the structure and kinematics of old Galactic subsystems – the halo and the thick disk. However, the number of RR Lyrae variables in the extended solar neighborhood with both precise multicolor photometry and bona fide radial velocities has for a long time been rather limited (Dambis et al. 2013) prompting us to initiate a program aimed at acquiring photometric observations and radial-velocity measurements for the greatest possible number of RR Lyraes. We published the first results of our photometric observations in our previous papers

*Email: leonid.berdnikov@gmail.com

(Berdnikov et al. 2011a, 2011b, 2012, 2014, 2016, 2020), where we suspected the presence of the Blazhko effect (Blazhko 1907) in several stars including SU Hor.

The aim of this study is to determine the period of the Blazhko effect and investigate the pulsation period stability of SU Hor.

2 Observational data

We performed Charge-Coupled Device (CCD) observations of SU Hor during four observing runs from December 2010 through January 2014 (JD 2455548 – 56679) with the 76-cm telescope of the South African Astronomical Observatory (SAAO) Sutherland in South Africa using SBIG CCD ST-10XME camera equipped with BVI_c-band filters of the Kron–Cousins system (Cousins 1976). A description of the technique used to reduce observing data can be found in our previous paper (Berdnikov et al. 2012). We acquired a total of 3201 CCD frames with photometric errors close to $0.^m01$. We already published observations from our first observing run in (Berdnikov et al. 2012), where we revealed the Blazhko effect in SU Hor.

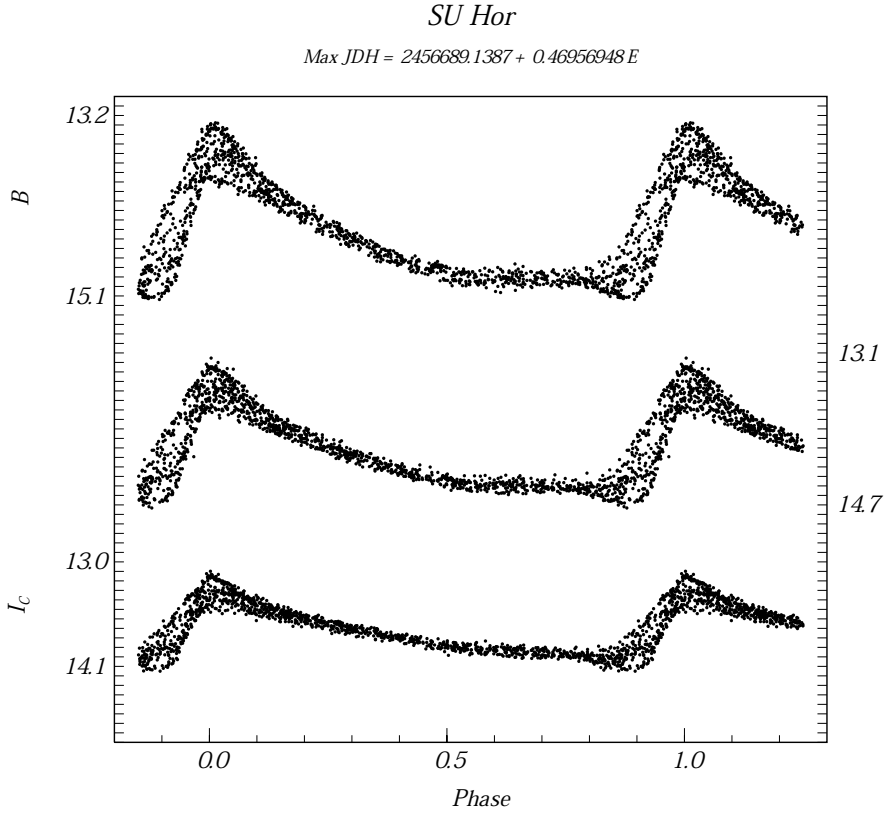


Figure 1 BVI_c-band phased light curves of the RR Lyrae type star SU Hor. The large scatter is due to the Blazhko effect.

We also used the Las Cumbres Observatory Global Telescope (LCOGT) Network (Brown et al. 2013) to acquire 1065 CCD BVI_c frames during the time interval JD 2456633–56689. We reduced LCOGT observations by performing differential photometry relative to secondary standards whose magnitudes we determined based on observations made in SAAO; the photometric errors of these observations, which were published in (Berdnikov et al. 2020), are close to $0.^m02$.

Figure 1 shows all our data plotted as phased light curves.

In addition to our own observations, we used 315 CCD observations from All Sky Automated Survey (ASAS-3) catalog (Pojmanski 2002) and 3900 observations from ASAS-SN catalog (Jayasinghe et al. 2019) as well as photographic photometry from Digital Access to a Sky Century at Harvard (DASCH) database of digitized astronomical plate data from Harvard University (Grindlay et al. 2009). Table 1 summarizes the information about the number of observations used.

The total time span of the data set used is 134 years.

Table 1 Observational data for SU Hor.

Data source	Number of observations	Type of observations	JD interval
DASCH (Grindlay et al., 2009)	895	Photogr. (PG)	2411611–2447145
ASAS-3 (Pojmanski, 2002)	315	CCD (V)	2451868–2455167
Berdnikov et al. (2012)	101	CCD (B)	2455548–2455567
Berdnikov et al. (2012)	100	CCD (V)	2455548–2455567
Berdnikov et al. (2012)	100	CCD (I_c)	2455548–2455567
Berdnikov et al. (2020)	1277	CCD (B)	2455896–2456689
Berdnikov et al. (2020)	1378	CCD (V)	2455896–2456689
Berdnikov et al. (2020)	1310	CCD (I_c)	2455896–2456689
ASAS-SN (Jayasinghe et al., 2019)	1054	CCD (V)	2457181–2458385
ASAS-SN (Jayasinghe et al., 2019)	2746	CCD (g)	2458012–2490719

3 Pulsation period changes

We investigate the pulsation period changes in SU Hor using the standard technique of the analysis of $O-C$ diagram. The most accurate technique for determining the $O-C$ residuals is the Hertzsprung method (Hertzsprung 1919) the computer implementation of which was described by Berdnikov (1992).

Table 2 lists the computed $O-C$ residuals of seasonal light curves of SU Hor. The first and second columns give the inferred time of maximum brightness and its standard error, respectively; the third column gives the type of observations used (see Table 2); the fourth and fifth columns give the number of epoch, E, and the $O-C$ residual (in days), and the sixth and seventh columns give the number of observations, N, and the data source (see Table 1), respectively. The data listed in Table 2 are shown in the O–C diagram (Fig. 2) by the circles; the vertical $O-C$ error bars are smaller than the symbols.

The $O-C$ diagram can be approximated by a cubic parabola:

$$\mathrm{Max\,JD_{hel}} = 2437605.9294 + 0.46974478\ E - 0.6055\ 10^{-9}\ E^2 - 0.2341\ 10^{-13}\ E^3 \quad (1),$$

$$\pm 0.0117 \quad \pm 0.561210^{-6} \quad \pm 0.118510^{-10} \quad \pm 0.3655\ 10^{-15}$$

which means that the period is decreasing at a rate of $dp/dt = -0.0814 \pm 0.0016$ s/year.

Table 2 Times of maximum brightness of SU Hor.

Max HJD	Error	Band	E	$O-C$, days	N	Data source
2414610.1032	0.0197	PG	−48956	0.9995	11	DASCH
2421795.6371	0.0103	PG	−33658	0.3776	11	DASCH
2424316.6005	0.0075	PG	−28291	0.2208	20	DASCH
2424348.5546	0.0047	PG	−28223	0.2322	21	DASCH
2424417.0923	0.0037	PG	−28077	0.1872	11	DASCH
2424823.4000	0.0034	PG	−27212	0.1657	21	DASCH
2425707.8775	0.0033	PG	−25329	0.1138	11	DASCH
2426342.4684	0.0072	PG	−23978	0.0795	15	DASCH
2427536.0440	0.0026	PG	−21437	0.0336	22	DASCH
2427545.4302	0.0035	PG	−21417	0.0249	23	DASCH
2428232.1545	0.0055	PG	−19955	−0.0177	15	DASCH
2428274.4058	0.0026	PG	−19865	−0.0434	45	DASCH
2428481.0828	0.0017	PG	−19425	−0.0542	86	DASCH
2428666.1578	0.0032	PG	−19031	−0.0586	43	DASCH
2428787.8284	0.0011	PG	−18772	−0.0519	291	DASCH
2428840.9037	0.0041	PG	−18659	−0.0578	10	DASCH
2429152.3333	0.0016	PG	−17996	−0.0690	33	DASCH
2429152.3334	0.0017	PG	−17996	−0.0688	33	DASCH
2429250.5071	0.0108	PG	−17787	−0.0718	15	DASCH
2429630.9855	0.0016	PG	−16977	−0.0867	68	DASCH
2429775.1763	0.0013	PG	−16670	−0.1076	120	DASCH
2429926.4170	0.0016	PG	−16348	−0.1246	20	DASCH
2430177.2443	0.0017	PG	−15814	−0.1410	39	DASCH
2430187.6116	0.0086	PG	−15792	−0.1082	22	DASCH
2430190.4192	0.0083	PG	−15786	−0.1190	11	DASCH
2430375.0356	0.0119	PG	−15393	−0.1124	9	DASCH
2430555.4186	0.0060	PG	−15009	−0.1113	16	DASCH
2431031.2418	0.0044	PG	−13996	−0.1396	8	DASCH
2431032.6137	0.0068	PG	−13993	−0.1769	9	DASCH
2432179.2534	0.0043	PG	−11552	−0.1842	18	DASCH
2432648.5242	0.0100	PG	−10553	−0.1885	25	DASCH
2432951.9816	0.0051	PG	−9907	−0.1863	18	DASCH
2443667.7699	0.0095	PG	12905	−0.2159	5	DASCH
2445412.2945	0.0066	PG	16619	−0.3234	15	DASCH
2445613.3172	0.0069	PG	17047	−0.3515	19	DASCH
2446261.0663	0.0028	PG	18426	−0.3804	8	DASCH
2446420.7477	0.0106	PG	18766	−0.4123	13	DASCH
2452245.2878	0.0016	V	31167	−1.1773	105	ASAS-3
2453418.3965	0.0023	V	33665	−1.4910	105	ASAS-3
2454525.2809	0.0029	V	36022	−1.7951	105	ASAS-3
2455558.8709	0.0009	B	38223	−2.1133	101	Berd2012
2455558.8724	0.0010	I_c	38223	−2.1118	100	Berd2012
2455558.8725	0.0010	V	38223	−2.1117	100	Berd2012
2455920.4606	0.0005	I_c	38993	−2.2271	426	Berd2020

Table 2 continued.

Max HJD	Error	Band	E	$O-C$, days	N	Data source
2455920.4609	0.0006	V	38993	−2.2269	491	Berd2020
2455922.8109	0.0006	B	38998	−2.2256	370	Berd2020
2456297.0551	0.0008	B	39795	−2.3679	308	Berd2020
2456298.9333	0.0008	I_c	39799	−2.3687	291	Berd2020
2456300.3434	0.0008	V	39802	−2.3679	281	Berd2020
2456642.1880	0.0009	B	40530	−2.4974	245	Berd2020
2456642.1890	0.0009	I_c	40530	−2.4964	245	Berd2020
2456642.1900	0.0010	V	40530	−2.4955	243	Berd2020
2456650.6429	0.0007	B	40548	−2.4980	354	Berd2020
2456651.5843	0.0007	V	40550	−2.4961	363	Berd2020
2456652.5215	0.0007	I_c	40552	−2.4984	348	Berd2020
2456968.9920	0.0016	V	41226	−2.6358	153	ASAS-SN
2457344.1583	0.0011	V	42025	−2.7956	300	ASAS-SN
2457693.0093	0.0010	V	42768	−2.9650	280	ASAS-SN
2458067.2073	0.0011	V	43565	−3.1536	213	ASAS-SN
2458083.1822	0.0019	g	43599	−3.1604	168	ASAS-SN
2458347.9710	0.0019	V	44163	−3.2973	108	ASAS-SN
2458458.3128	0.0009	g	44398	−3.3559	644	ASAS-SN
2458798.2372	0.0007	g	45122	−3.5267	799	ASAS-SN
2459179.9591	0.0009	g	45935	−3.7073	491	ASAS-SN
2459401.1162	0.0015	g	46406	−3.8000	90	ASAS-SN
2459561.2330	0.0018	g	46747	−3.8662	132	ASAS-SN
2459867.8937	0.0012	g	47400	−3.9488	96	ASAS-SN
2460284.0067	0.0009	g	48286	−4.0297	198	ASAS-SN
2460601.0418	0.0011	g	48961	−4.0723	128	ASAS-SN

Note: Berd2012, Berdnikov et al. (2012); Berd2020, Berdnikov et al. (2020).

To confirm that the changes in the pulsation period are real, we use the method proposed by Lombard and Koen (1993). To this end, we calculated the differences $\Delta(O-C)_i$ of the successive $O-C$ residuals from Table 2, $\Delta(O-C)_i = (O-C)_{i+1} - (O-C)_i$, and plotted $P'_i = \Delta(O-C)_i/(E_{i+1}-E_i)$ against $E'_i = (E_i+E_{i+1})/2$ (Fig. 3). P'_i, which have the meaning of the mean period in an epoch interval $E_i - E_{i+1}$, correspond to the behavior of the $O-C$ residuals in Fig. 2.

We found, based on our CCD observations, that maxima in the B-band filter occur $0.^d0016$ before the corresponding maxima in the V-band filter, and maxima in the V-band filter occur $0.^d0009$ before the corresponding maxima in the I_c-band filter. We applied these corrections when constructing the $O-C$ diagram in Fig. 2 and determined ephemeris (1), which therefore refers to the V-band light curve.

Note that the results concerning period changes that we report in this paper are based on concrete light-curve templates adopted from Berdnikov (2020) and shown graphically in Fig. 3.

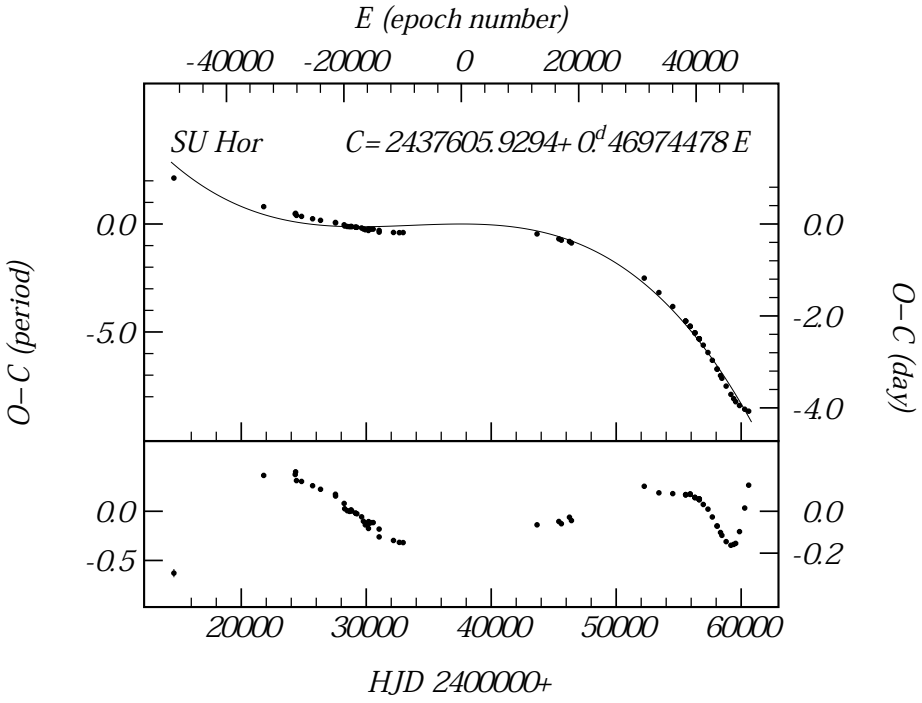


Figure 2 $O - C$ diagram of SU Hor.

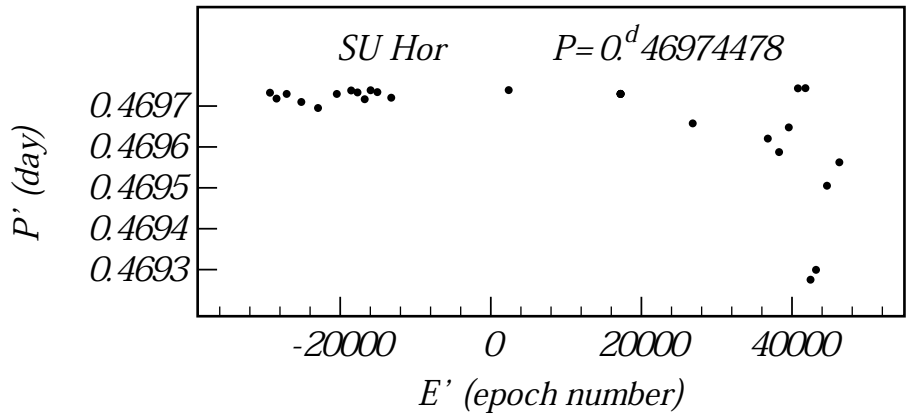


Figure 3 $P'_i = ((O-C)_{i+1} - (O-C)_i)/(E_{i+1} - E_i)$ vs $E'_i = (E_i + E_{i+1})/2$. P'_i, which have the meaning of the mean period in an epoch interval $E_i - E_{i+1}$, correspond to the behavior of the $O - C$ residuals in Fig. 2.

4 The Blazhko effect

To determine the period of the Blazhko effect, we used the method developed by Goranskij (1976), which consists in the following. Magnitudes are converted to intensities and for each trial period P_{Bl} of the Blazhko effect all observations are subdivided into (in our case) 10 equal phase intervals, and inside each such interval observations are sorted by the phase of the main period. The total scattering parameter S_N is computed, which is equal to the normalized sum of squared deviations of each successive point of the combined light curve from the previous point (in terms of phase). In the case of the true P_{Bl} (or frequency F_{Bl}) observations in each of the 10 intervals (Fig. 4) are practically unaffected by the scattering due to the Blazhko effect and therefore the scattering parameter S_N is minimal.

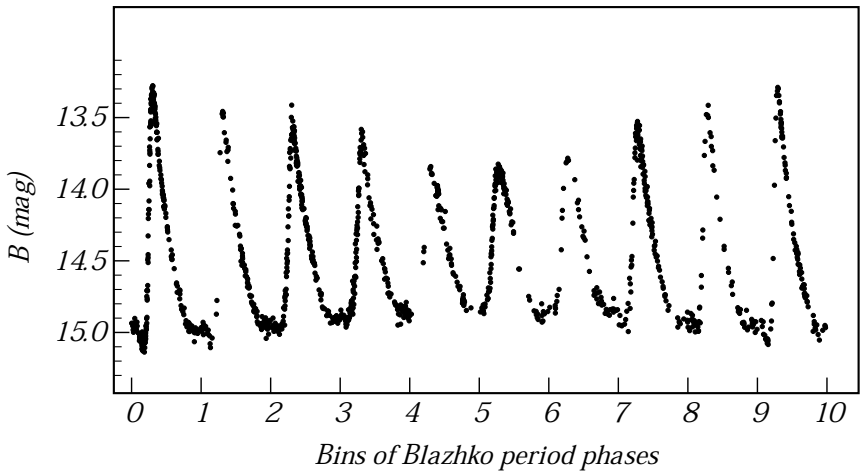


Figure 4 B-band phased light curves of SU Hor in 10 narrow successive bins of Blazhko period ($P_{Bl} = 32.^d276$) phases.

The scattering parameter for 1277 B-band observations (Fig. 5) reaches its minimum value at P_{Bl} close to $32.^d276$ ($F_{Bl} = 0.0309825$). For 1378 V- and 1310 I_c-band observations, the Blazhko period estimates are $32.^d288$ ($F_{Bl} = 0.0309715$) and $32.^d265$ ($F_{Bl} = 0.0309934$), respectively.

We also used PERIOD04 program (Lenz and Breger 2005) to compute frequency spectra. The most prominent frequencies are listed in Table 3. The dependence of their amplitudes on harmonic order shown in Fig. 6 agrees with the results obtained for other Blazhko stars (Kolenberg 2009, 2011).

The 36 triplet components of the first six harmonics yield the mean Blazhko frequency of 0.031025 d^{-1}, corresponding to the Blazhko period of $32.^d232$.

Hence the mean Blazhko period averaged over both methods employed is $32.^d27 \pm 0.^d03$.

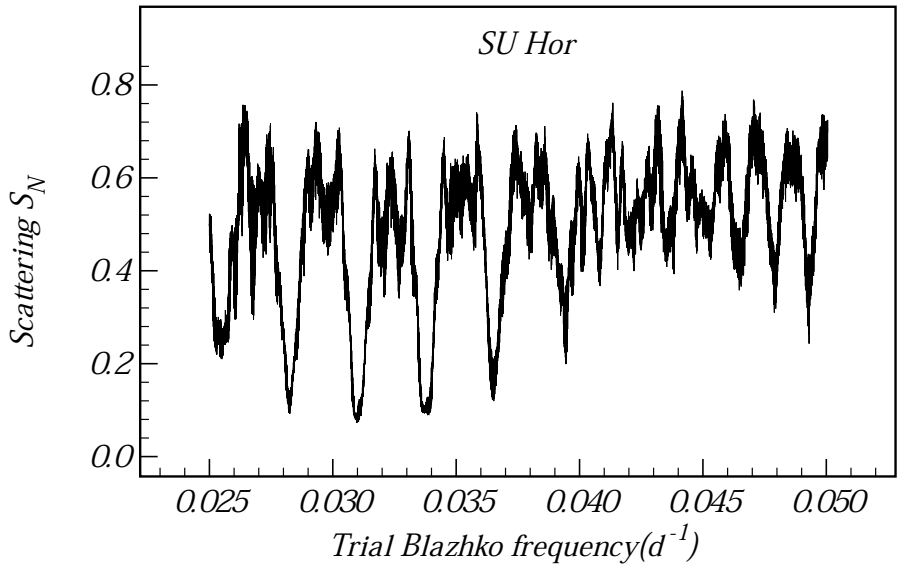


Figure 5 Dependence of the normalized scattering parameter S_N on the trial Blazhko frequency F_{Bl} for B-band observations of SU Hor. S_N reaches a minimal value at $F_{Bl} = 0.0309825$ (P_{Bl} is $32.^d276$).

Table 3 Amplitudes and phases of the pulsation and modulation frequency components of SU Hor.

Filter	Name of frequency	Frequency (d^{-1})	Amplitude (mag)	Phase ($rad/2\pi$)
B	$f_0 - 2F_{Bl}$	2.0672535±0.0000934	0.0097±0.0015	0.3504±0.0213
B	$f_0 - F_{Bl}$	2.0984180±0.0000340	0.0269±0.0016	0.5800±0.0077
V	$f_0 - F_{Bl}$	2.0984829±0.0000469	0.0175±0.0014	0.9196±0.0107
I_c	$f_0 - F_{Bl}$	2.0985543±0.0000530	0.0138±0.0012	0.9152±0.0121
I_c	f_0	2.1296113±0.0000029	0.2486±0.0012	0.7824±0.0006
B	f_0	2.1296151±0.0000017	0.5306±0.0016	0.6040±0.0003
V	f_0	2.1296154±0.0000020	0.4032±0.0013	0.5818±0.0004
V	$f_0 + F_{Bl}$	2.1605969±0.0000113	0.0729±0.0014	0.4795±0.0025
B	$f_0 + F_{Bl}$	2.1606006±0.0000098	0.0928±0.0017	0.2706±0.0022
I_c	$f_0 + F_{Bl}$	2.1606605±0.0000164	0.0446±0.0012	0.9036±0.0037
B	$f_0 + 2F_{Bl}$	2.1918050±0.0001155	0.0079±0.0017	0.7127±0.0264
V	$f_0 + 2F_{Bl}$	2.1919119±0.0001119	0.0073±0.0013	0.6561±0.0256
B	$2f_0 - 2F_{Bl}$	4.1974393±0.0001333	0.0068±0.0016	0.4132±0.0305
V	$2f_0 - F_{Bl}$	4.2281825±0.0000398	0.0207±0.0013	0.0746±0.0091
I_c	$2f_0 - F_{Bl}$	4.2282141±0.0000480	0.0153±0.0012	0.3058±0.0110
B	$2f_0 - F_{Bl}$	4.2282390±0.0000348	0.0262±0.0017	0.9028±0.0079

Table 3 continued.

Filter	Name of frequency	Frequency (d^{-1})	Amplitude (mag)	Phase ($rad/2\pi$)
I_c	$2f_0$	4.2592062±0.0000064	0.1137±0.0012	0.9006±0.0014
B	$2f_0$	4.2592111±0.0000040	0.2233±0.0016	0.6304±0.0009
V	$2f_0$	4.2592165±0.0000046	0.1762±0.0013	0.3285±0.0010
V	$2f_0 + F_{Bl}$	4.2902179±0.0000148	0.0556±0.0013	0.1104±0.0033
B	$2f_0 + F_{Bl}$	4.2902367±0.0000126	0.0724±0.0016	0.0473±0.0028
I_c	$2f_0 + F_{Bl}$	4.2902568±0.0000215	0.0341±0.0012	0.9181±0.0049
B	$2f_0 + 2F_{Bl}$	4.3214464±0.0004071	0.0022±0.0017	0.9192±0.0931
V	$2f_0 + 2F_{Bl}$	4.3215746±0.0001550	0.0053±0.0012	0.8818±0.0355
B	$3f_0 - 2F_{Bl}$	6.3263768±0.0003210	0.0028±0.0016	0.5937±0.0734
B	$3f_0 - F_{Bl}$	6.3578260±0.0000302	0.0302±0.0016	0.5329±0.0069
I_c	$3f_0 - F_{Bl}$	6.3578354±0.0000439	0.0167±0.0012	0.0187±0.0100
V	$3f_0 - F_{Bl}$	6.3578398±0.0000325	0.0253±0.0013	0.7538±0.0074
V	$3f_0$	6.3888131±0.0000073	0.1126±0.0013	0.3704±0.0016
I_c	$3f_0$	6.3888160±0.0000100	0.0728±0.0012	0.2078±0.0023
B	$3f_0$	6.3888213±0.0000065	0.1400±0.0016	0.9054±0.0014
B	$3f_0 + F_{Bl}$	6.4198384±0.0000135	0.0674±0.0017	0.8123±0.0031
I_c	$3f_0 + F_{Bl}$	6.4198467±0.0000208	0.0353±0.0012	0.3501±0.0047
V	$3f_0 + F_{Bl}$	6.4198662±0.0000151	0.0544±0.0013	0.2433±0.0034
B	$3f_0 + 2F_{Bl}$	6.4507886±0.0000755	0.0121±0.0017	0.3725±0.0172
B	$4f_0 - 2F_{Bl}$	8.4563848±0.0001616	0.0056±0.0016	0.1688±0.0369
V	$4f_0 - F_{Bl}$	8.4873279±0.0000420	0.0196±0.0013	0.8969±0.0096
I_c	$4f_0 - F_{Bl}$	8.4873599±0.0000536	0.0137±0.0012	0.1354±0.0122
B	$4f_0 - F_{Bl}$	8.4873767±0.0000350	0.0261±0.0016	0.1389±0.0080
I_c	$4f_0$	8.5184236±0.0000171	0.0427±0.0012	0.6464±0.0039
V	$4f_0$	8.5184268±0.0000126	0.0652±0.0013	0.4637±0.0028
B	$4f_0$	8.5184302±0.0000112	0.0812±0.0016	0.2722±0.0025
B	$4f_0 + F_{Bl}$	8.5494324±0.0000158	0.0578±0.0016	0.9891±0.0036
I_c	$4f_0 + F_{Bl}$	8.5494333±0.0000237	0.0309±0.0012	0.9589±0.0054
V	$4f_0 + F_{Bl}$	8.5494428±0.0000182	0.0453±0.0013	0.4132±0.0041
B	$4f_0 + 2F_{Bl}$	8.5804647±0.0001896	0.0048±0.0016	0.0468±0.0433
I_c	$5f_0 - F_{Bl}$	10.6168503±0.0001657	0.0044±0.0012	0.1736±0.0379
V	$5f_0 - F_{Bl}$	10.6171038±0.0000797	0.0103±0.0013	0.8322±0.0182
B	$5f_0 - F_{Bl}$	10.6171204±0.0000928	0.0098±0.0016	0.9196±0.0212
B	$5f_0$	10.6480092±0.0000196	0.0466±0.0016	0.2853±0.0044
V	$5f_0$	10.6480468±0.0000212	0.0387±0.0013	0.1779±0.0048
I_c	$5f_0$	10.6480779±0.0000261	0.0281±0.0012	0.4207±0.0059
I_c	$5f_0 + F_{Bl}$	10.6790248±0.0000324	0.0226±0.0012	0.3021±0.0074
V	$5f_0 + F_{Bl}$	10.6790505±0.0000227	0.0363±0.0013	0.8632±0.0052
B	$5f_0 + F_{Bl}$	10.6790540±0.0000203	0.0450±0.0015	0.6494±0.0046
I_c	$5f_0 + 2F_{Bl}$	10.7102104±0.0000809	0.0090±0.0011	0.7393±0.0185

Table 3 continued.

Filter	Name of frequency	Frequency (d^{-1})	Amplitude (mag)	Phase ($rad/2\pi$)
B	$6f_0 - F_{Bl}$	12.7465223±0.0000869	0.0105±0.0015	0.8488±0.0198
V	$6f_0 - F_{Bl}$	12.7466537±0.0001054	0.0078±0.0013	0.4866±0.0241
I_c	$6f_0 - F_{Bl}$	12.7467505±0.0001823	0.0040±0.0012	0.0487±0.0417
I_c	$6f_0$	12.7776162±0.0000614	0.0119±0.0012	0.7481±0.0140
B	$6f_0$	12.7776209±0.0000314	0.0291±0.0016	0.4843±0.0071
V	$6f_0$	12.7776492±0.0000417	0.0198±0.0013	0.9020±0.0095
V	$6f_0 + F_{Bl}$	12.8086665±0.0000310	0.0266±0.0013	0.7966±0.0070
I_c	$6f_0 + F_{Bl}$	12.8086757±0.0000426	0.0172±0.0012	0.2988±0.0097
B	$6f_0 + F_{Bl}$	12.8087012±0.0000281	0.0325±0.0016	0.8456±0.0064
B	$7f_0 - F_{Bl}$	14.8760930±0.0001145	0.0079±0.0015	0.4368±0.0262
I_c	$7f_0 - F_{Bl}$	14.8762760±0.0001624	0.0045±0.0012	0.1798±0.0371
V	$7f_0 - F_{Bl}$	14.8763357±0.0001892	0.0043±0.0013	0.8231±0.0433
V	$7f_0$	14.9070435±0.0000843	0.0097±0.0013	0.2651±0.0193
I_c	$7f_0$	14.9072454±0.0000893	0.0082±0.0012	0.9447±0.0204
B	$7f_0$	14.9073316±0.0000675	0.0135±0.0015	0.1168±0.0154
I_c	$7f_0 + F_{Bl}$	14.9382210±0.0000572	0.0128±0.0012	0.2145±0.0131
B	$7f_0 + F_{Bl}$	14.9382605±0.0000361	0.0253±0.0015	0.9946±0.0082
V	$7f_0 + F_{Bl}$	14.9383188±0.0000369	0.0223±0.0013	0.7308±0.0084
B	$8f_0 - F_{Bl}$	17.0057345±0.0001207	0.0075±0.0015	0.8813±0.0276
V	$8f_0 - F_{Bl}$	17.0057654±0.0001040	0.0079±0.0013	0.1729±0.0238
I_c	$8f_0 - F_{Bl}$	17.0057964±0.0001467	0.0050±0.0011	0.4905±0.0335
I_c	$8f_0$	17.0366279±0.0001618	0.0045±0.0012	0.9872±0.0370
V	$8f_0$	17.0368096±0.0001089	0.0075±0.0013	0.7833±0.0249
B	$8f_0$	17.0368264±0.0001158	0.0079±0.0016	0.7930±0.0265
I_c	$8f_0 + F_{Bl}$	17.0679546±0.0000630	0.0116±0.0012	0.5269±0.0144
B	$8f_0 + F_{Bl}$	17.0680179±0.0000543	0.0168±0.0015	0.9864±0.0124
V	$8f_0 + F_{Bl}$	17.0706938±0.0000649	0.0127±0.0013	0.3460±0.0148
V	$9f_0 - F_{Bl}$	19.1353557±0.0004166	0.0019±0.0013	0.5740±0.0953
B	$9f_0$	19.1663064±000099042	0.0092±0.0015	0.3576±0.0226
V	$9f_0$	19.1663945±0.0001434	0.0057±0.0013	0.4305±0.0328
I_c	$9f_0$	19.1664690±0.0001677	0.0043±0.0011	0.2265±0.0383
I_c	$9f_0 + F_{Bl}$	19.1974421±0.0000867	0.0084±0.0015	0.7259±0.0198
V	$9f_0 + F_{Bl}$	19.1975248±0.0000709	0.0116±0.0013	0.0881±0.0162
B	$9f_0 + F_{Bl}$	19.1975251±0.0000912	0.0100±0.0016	0.0538±0.0208
B	$9f_0 + 2F_{Bl}$	19.2285240±0.0001058	0.0086±0.0014	0.9857±0.0242
B	$10f_0 + F_{Bl}$	21.3271037±000083202	0.0110±0.0015	0.1148±0.0190

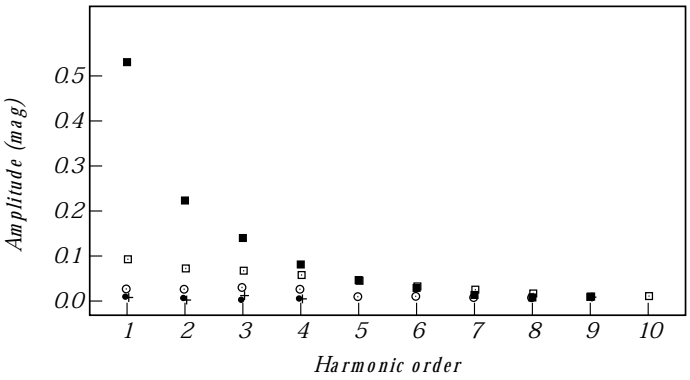


Figure 6 B-band amplitudes from Table 6 vs harmonic order. Filled squares are harmonics, open circles and squares are left and right triplet components, filled circles and plus signs are left and right quintuplet components.

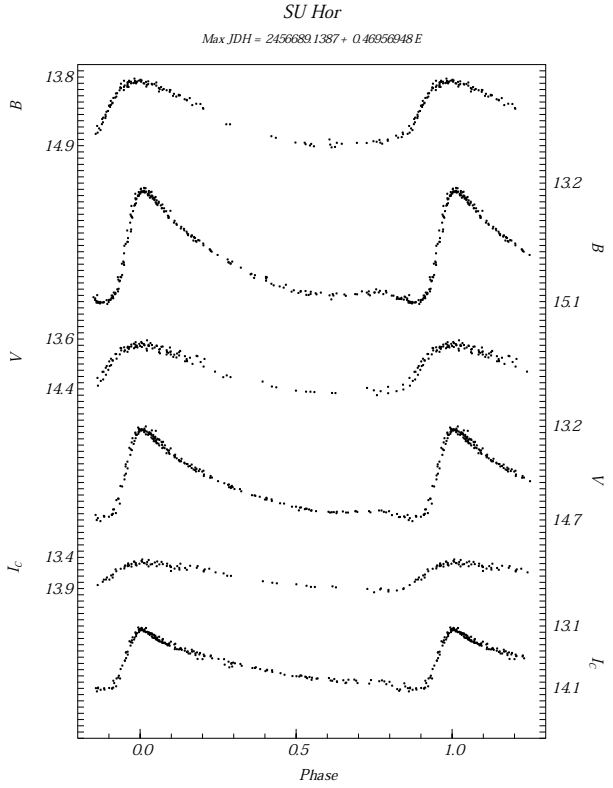


Figure 7 B-, V- and I_c-band phased light curves of SU Hor in narrow Blazhko phase bins corresponding to the maximum and minimum amplitude.

Figure 7 shows the B-, V- and I_c-band light curves of SU Hor folded with the pulsation period for observations in the narrow bins of P_{Bl} phases corresponding to the maximum and minimum amplitudes.

5 Conclusions

1. We acquired 3965 CCD frames in the BVI_c-band filters for the RR Lyrae type variable SU Hor. Our observations resulted in a phased light curve with a large scatter, especially near maximum brightness, which allowed us to confirm the Blazhko effect, which we suspected in our previous paper.
2. Our observations allowed us to determine the period of the Blazhko effect, $P_{Bl} = 32.^d27 \pm 0.^d03$.
3. We constructed the $O - C$ diagram for SU Hor, which spans a 134-year long time interval, allowing us to reveal for the first time the evolutionary period change at a rate of $dp/dt = -0.0814 \pm 0.0016$ s/year.

6 Acknowledgments

The study was conducted under the state assignment of Lomonosov Moscow State University. This work makes use of observations from the LCOGT network, from the South African Astronomical Observatory (SAAO) Sutherland, and data from the ASAS, ASAS-SN and DASCH projects.

References

Berdnikov L.N. (1992) SvAL **18**, 207.
Berdnikov L.N., Kniazev A.Yu., Sefako R., et al. (2011a) The Observatory **131**, 315
Berdnikov L.N., Kniazev A.Yu., Sefako R., et al. (2011b) The Observatory **131**, 386
Berdnikov L.N., Vozyakova O.V., Kniazev A.Yu., et al. (2012) ARep,**56**, 290
Berdnikov L.N., Kniazev A.Yu., Sefako R., et al. (2014) The Observatory **134**, 206
Berdnikov L.N., Kniazev A.Yu., Dambis A.K., et al. (2016) ApSS **361**, 320
Berdnikov L.N., Kniazev A.Yu., Dambis A.K., et al. (2020) Peremennye Zvezdy (Variable Stars) **40**, No. 9
Blazhko S. (1907) AN **175**, 325
Brown T.M., Baliber N., Bianco F.B., et al. (2013) PASP **125**, 1031
Cousins A.W.J. (1976) Mem. RAS **81**, 25.
Dambis A.K., Berdnikov L.N., Kniazev A.Yu., et al. (2013) MNRAS **435**, 3206
Goranskij V.P. (1976) Peremennye Zvezdy, Prilozh. **2**, 323
Grindlay J., Tang S., Simcoe R., et al. (2009) In: Preserving Astronomy's Photographic Legacy. ASP Conf. Ser., vol. 410, 101
Hertzsprung E. (1919) AN **210**, 17
Jayasinghe T., Stanek K.Z., Kochanek C.S., et al. (2019) MNRAS **485**, 961
Kolenberg K., Guggenberger E., Medupe T., et al. (2009) MNRAS **396**, 263

Kolenberg K., Bryson S., Szabo R., et al. (2011) MNRAS **411**, 878
Lenz P. and Breger M. (2005) Comm. in Asteroseismology **146**, 53
Lombard F. and Koen C. (1993) MNRAS **263**, 309
Pojmanski G. (2002) AcA **52**, 397